JOURNAL OF VIROLOGY, June 1995, p. 3560–3574 Vol. 69, No. 6
0022-538X/95/$04.00+0

Assembly of Vaccinia Virus: Incorporation of p14 and p32 into the Membrane of the Intracellular Mature Virus

BEATE SODEIK,[1]† SALLY CUDMORE,[1] MARIA ERICSSON,[1] MARIANO ESTEBAN,[2] EDWARD G. NILES,[3] AND GARETH GRIFFITHS[1]*

Cell Biology Program, European Molecular Biology Laboratory, 69012 Heidelberg, Germany[1]; Centro Nacional de Biotecnologia, Consejo Superior de Investigaciones, Científicas, Campus Universidad Autonoma, 28049 Madrid, Spain[2]; and Department of Biochemistry, School of Medicine, State University of New York, Buffalo, New York 14214[3]

Received 9 June 1994/Accepted 14 March 1995

The cytoplasmic assembly of vaccinia virus begins with the transformation of a two-membraned cisterna derived from the intermediate compartment between the endoplasmic reticulum and the Golgi complex. This cisterna develops into a viral crescent which eventually forms a spherical immature virus (IV) that matures into the intracellular mature virus (IMV). Using immunoelectron microscopy, we determined the subcellular localization of p32 and p14, two membrane-associated proteins of vaccinia virus. p32 was associated with vaccinia virus membranes at all stages of virion assembly, starting with the viral crescents, as well as with the membranes which accumulated during the inhibition of assembly by rifampin. There was also low but significant labelling of membranes of some cellular compartments, especially those in the vicinity of the Golgi complex. In contrast, anti-p14 labelled neither the crescents nor the IV but gave strong labelling of an intermediate form between IV and IMV and was then associated with all later viral forms. This protein was also not significantly detected on identifiable cellular membranes. Both p32 and p14 were abundantly expressed on the surface of intact IMV. Our data are consistent with a model whereby p32 would become inserted into cellular membranes before being incorporated into the crescents whereas p14 would be posttranslationally associated with the viral outer membrane at a specific later stage of the viral life cycle.

Vaccinia virus is the best-studied member of the family *Poxviridae*, the largest and most complex of the animal viruses (for reviews, see references 5, 13, 18, and 28). Vaccinia virus replication and assembly occur in discrete cytoplasmic foci termed viral factories (1, 4, 24). The first morphological evidence for viral assembly is the formation of crescent-shaped membranes. On the basis of immunoelectron microscopy with antibodies specific to cellular membranes, in conjunction with a lipid analysis of purified virions, we have shown that these viral crescents are derived from a membrane cisterna of the intermediate compartment, which is located between the endoplasmic reticulum (ER) and the Golgi stacks (45). Our data also argue that the crescents are made up of two closely apposed membranes rather than one (45), as previous studies had suggested (5). The viral crescents eventually form spherical, immature virions which undergo additional maturational events such as proteolytic cleavages (5, 29), to give rise to the brick-shaped form of vaccinia virus, designated the intracellular naked virus (19, 31) or intracellular mature virus (IMV) (45). Data from both thawed cryosections of aldehyde-fixed vaccinia virus-infected cells (45) and cryoelectron microscopy (cryo-EM) of purified, frozen hydrated IMV (9) have also argued that the IMV contains at least two membranes. A fraction of the IMV becomes enwrapped by an additional cisterna, derived from the trans-Golgi network, thereby forming the intracellular enveloped virus (IEV), a form enveloped by four membranes (44). The outermost membrane of the IEV is thought to fuse with the plasma membrane, thereby releasing the extracellular enveloped virus (EEV), containing one fewer membrane than the IEV (44), into the medium (36).

By two-dimensional gel electrophoresis, purified IMVs have been shown to contain at least 111 different polypeptides (12). According to their solubility under reducing conditions in Nonidet P-40 (NP-40) or Triton X-100, the proteins of the IMV were classified into core proteins and envelope proteins (11, 21, 23, 34, 43). Envelope proteins of the IMV were also identified by surface labelling, by their accessibility to proteases on the surface of purified IMV, or by their capability to induce neutralizing antibodies against the IMV (3, 34, 35, 39, 47).

Probably the two best-characterized membrane proteins of the IMV are p32, encoded by the gene D8L (27, 32), and p14, encoded by the gene A27L (38). p32 was one of the first putative integral membrane proteins identified as being incorporated into the IMV. It has a molecular mass of 32 kDa, a C-terminal hydrophobic membrane anchor predicted from its sequence, and 36% homology to carbonic anhydrase. It is not glycosylated and is nonessential for the viral life cycle in cultured cells (32, 42). Further, p32 binds specifically to the plasma membrane. Inactivation of the gene results in reduced levels of gene expression and alternation of the virus, probably because of a function of p32 during virus entry (42). That deletion of p32 does not inhibit entry may be explained by redundancy: it seems likely that more than one protein can function as a ligand for the cellular receptors that facilitate entry.

p14 was first identified with a monoclonal antibody which neutralized IMV infectivity (6, 39). This 14-kDa protein has been postulated to exist as disulfide-linked trimers within the virus and to be involved in the fusion of the IMV with the plasma membrane upon virus entry, as well as in cell-cell fusion (16, 40). When p14 synthesis is repressed during the viral life cycle, normal infectious IMVs are formed, but they are not

* Corresponding author. Mailing address: EMBL, Meyerhofstr. 1, Postfach 10.2209, 69012 Heidelberg, Germany. Phone: 49-6221-387267. Fax: 49-6221-387306.

† Present address: Department of Cell Biology, Yale University School of Medicine, New Haven, CT 06520-8002.

wrapped by intracellular membranes and no IEVs or EEVs are formed (41). Thus, in contrast to p32, p14 is essential for the assembly of the IEV and consequently for the EEV.

While the protein composition of both IMV and EEV has been relatively well characterized, little is known about the proteins present in the immature viral structures because these particles have not been purified. Immunogold EM offers an alternative approach for asking whether or not a particular protein is enriched in the various morphological forms of the virus. With this rationale, we began a detailed analysis of the distribution of several vaccinia virus structural proteins (44–46). In this paper, we describe the subcellular localization of two vaccinia virus membrane proteins, p14 and p32. Our data show that p32 is associated with all morphologically detectable forms of the virus from the crescents onwards. In contrast, p14 is first detected on viral membranes at a later step during the transition from the intracellular immature virus (IV) to the IMV.

MATERIALS AND METHODS

Materials. Tissue culture reagents were obtained from Gibco BRL (Gaithersburg, Md.). HeLa cells (ATCC CCL 2) were grown in Eagle's minimal essential medium supplemented with 10% fetal calf serum (heat inactivated) and nonessential amino acids, and BHK-21 cells (ATCC CCL 10) were grown in Glasgow's modified Eagle's medium supplemented with 5% fetal calf serum and 10% tryptose phosphate broth. All media contained 2 mM glutamine, 100 U of penicillin per ml, and 10 mg of streptomycin per ml, and all cell lines were grown as adherent cultures in a 5% CO_2 incubator at 37°C. Virus propagation and titration with the vaccinia virus strain WR (ATCC VR 1354), kindly provided by B. Moss (National Institutes of Health, Bethesda, Md.), were performed as previously described (10). We used two rabbit antibodies (D8.1 and D8.2) raised against a region of p32 (gene D8L) consisting of amino acids 77 to 294 (32). We also used two antibodies against p14 (gene A27L), a mouse monoclonal antibody (C3) (39), and a rabbit antipeptide antibody (C4) raised against the first 20 amino acids of the N terminus of p14 (6). All secondary antibodies, rhodamine-coupled goat anti-rabbit or goat anti-mouse antibodies, and rabbit anti-mouse immunoglobulin G were obtained from Organon Teknika/Cappel (West Chester, Pa.).

Virus infections and drug treatments. Cells were grown for 2 days to approximately 90% confluency, washed once in phosphate-buffered saline (PBS), and then infected in serum-free Eagle's minimal essential medium at a multiplicity of infection of 10 to 20 PFU per cell (7). After 1 h at 37°C with intermittent agitation, the inoculum was aspirated off and the cells were placed in normal growth medium at 37°C with or without rifampin (final concentration, 100 μg/ml; Sigma, St. Louis, Mo.). Rifampin was stored as a 1,000-fold stock solution in dimethyl sulfoxide at −20°C. For chase experiments, the cells were washed three times with ice-cold PBS at the indicated times and then further incubated with prewarmed, normal rifampin-free medium at 37°C.

Microscopy. Vaccinia virus-infected HeLa and BHK cells were processed for microscopy as previously described (44–46). Briefly, for immunofluorescence experiments all incubations were carried out with PBS, pH 7.4, as a buffer. The cells were fixed with 3% paraformaldehyde for 20 min, quenched with 50 mM NH_4Cl for 10 min, and then permeabilized in 0.2% Triton X-100 for 4 min. They were labelled with the first antibody and subsequently with fluorescently labelled secondary antibodies, both in 0.2% gelatin for 20 min. Nuclear and viral DNAs were stained with 5 μg of *bis*-benzimide per ml (Hoechst no. 33258; Sigma) for 5 min. The coverslips were mounted in moviol on glass slides, examined with an Axiophot microscope (Carl Zeiss, Oberkochen, Germany), and photographed with TMAX Kodak film (ASA 400). For immunogold labelling on thawed cryosections, the cells were removed from the culture dish by proteinase K (25 μg/ml for HeLa cells and 50 μg/ml for BHK cells in 0.25 M HEPES [*N*-2-hydroxyethylpiperazine-*N*′-2-ethanesulfonic acid], pH 7.4) on ice for 2 to 3 min and fixed in 8% paraformaldehyde in 0.25 M HEPES, pH 7.4, overnight. Cell pellets were infiltrated with 2.1 M sucrose in PBS, frozen, and stored in liquid nitrogen. Ultrathin sections were cut at −90°C, transferred to Formvar-coated grids, and labelled (with protein A gold) and contrasted as described previously (17). The sequential procedure for double labelling is also described in reference 17. The treatment of cells with streptolysin O (SLO) (Wellcome Diagnostics, Dartford, United Kingdom) and their preparation for cryosectioning are described in reference 25.

For labelling whole virus, purified IMV was adsorbed onto glow-discharged grids that had been coated with Formvar and carbon. Grids with adsorbed virus were then treated with (i) NP-40 (1%) and dithiothreitol (DTT) (20 mM) for 30 min at 37°C, (ii) DTT alone (20 mM) at 37°C, (iii) trypsin (50 μg/ml) at 37°C, or (iv) proteinase K (50 μg/ml) at 4°C. Subsequently, the grids were rinsed with PBS, blocked for 10 min with 1% fetal calf serum, and labelled with either anti-p14 (followed by rabbit anti-mouse antibody) or anti-p32. The bound antibodies were visualized by protein A-gold (10 min). Following extensive rinses with PBS (20 min), the grids were rinsed with three changes (30 s total) of triple-distilled water and floated on 2% uranyl acetate for 30 s, and following removal of excess stain with filter paper, the grids were air dried.

RESULTS

Localization of p32. We began our analysis with p32, which is present in purified IMV and for which a transmembrane domain has been postulated on the basis of its predicted amino acid sequence (32). The two p32 antibodies that we used (32) gave identical results. By immunofluorescence microscopy at 8 h postinfection, anti-p32 strongly labelled the region of the viral factories (45, 46) (Fig. 1b) as defined by DNA staining (Fig. 1a, arrowheads). Additionally, there was strong labelling of punctate structures scattered throughout the whole cytoplasm and a weaker reticular labelling extending out to the periphery of the cells (Fig. 1b). We suggest that the punctate structures are IMV particles while the reticular labelling represents the ER. When the infection was carried out for 8 h in the presence of rifampin (30), anti-p32 labelled ring-shaped structures (Fig. 1e) which corresponded to the boundaries of the rifampin bodies, which we identified with phase-contrast microscopy (45, 46) (arrowheads in Fig. 1f). Additionally, we observed the same reticular labelling throughout the whole cytoplasm that was seen without rifampin. Both with and without rifampin, there was no labelling of the plasma membrane.

On ultrathin thawed cryosections of vaccinia virus-infected cells, anti-p32 labelled all identifiable forms of the virus (Fig. 2 to 5). Significant labelling for p32 was seen over the peripheral regions of many of the IVs (Fig. 4 and 5), the electron-dense intermediate form between the IV and the IMV (see references 45 and 46) (Fig. 2e and f), and the IMV particles (Fig. 2a to d, 3, and 4) which were strongly labelled on their membranes. The majority of label was associated with the outer of the two viral membranes of the IMV, but on many profiles of the IMV, the gold particles were also found over the inner membranes (Fig. 2b, c, and e). In the IEV, the second membrane and occasionally the inner membranes but in general not the two outermost membranes were labelled (Fig. 2g). There was also low but consistent labelling associated with the periphery of the Golgi stacks (Fig. 3). The central parts of the Golgi stacks (Fig. 3) and the plasma membrane (Fig. 2g) were essentially unlabelled. We also detected a low but significant labelling of the rough ER and the nuclear envelope (Fig. 4).

By evaluating a large number of preparations, it was clear that, on average, all viral forms were strongly labelled. However, for all forms individual examples that had low or no labelling were commonly seen (e.g., Fig. 3b). In our experience, such differences are often caused by variability in the access of antibodies to their antigens in the cryosections. Access is often improved on the surface of thawed cryosections from cells which were permeabilized with the bacterial, pore-forming toxin SLO prior to fixation (25). We therefore prepared HeLa cells infected with vaccinia virus (8 h) according to the same protocol. As shown in Fig. 5, after SLO extraction there was significantly more labelling of the IV (Fig. 5) and possibly of IMV (not shown). Not only the membranes of the IV but also those of the crescent were uniformly accessible for labelling with both peptide antibodies against p32. Moreover, labelled membranes that are apparently partially enclosed by the cup-shaped crescent structures were often seen (seen in section on the left of one crescent in Fig. 5b [arrowheads]). The significance of these internal membranes must await a more detailed study of the assembly process.

When cells were infected in the presence of rifampin, the viral precursor membranes surrounding the rifampin bodies

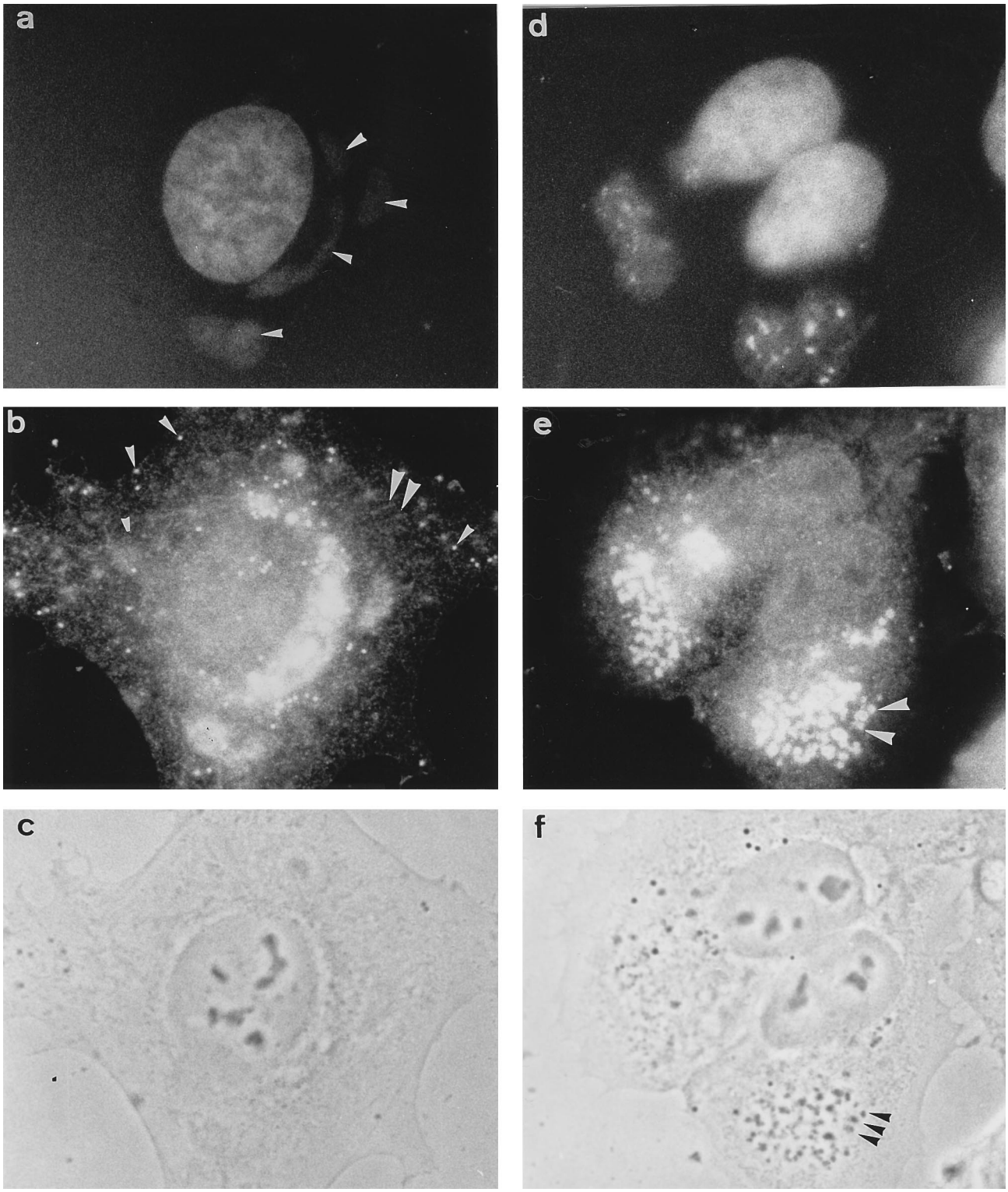

FIG. 1. Localization of p32 by immunofluorescence. Shown are vaccinia virus-infected HeLa cells 8 h postinfection in the absence (a to c) or presence (d to f) of rifampin. The cells were labelled with a fluorescent DNA dye (a and d) and with anti-p32 followed by rhodamine-conjugated goat anti-rabbit antibody (b and e). Panels c and f show the corresponding phase-contrast images. In the absence of rifampin, anti-p32 (b) shows a strong labelling in the region of the viral factories as defined by DNA staining (arrowheads in panel a). Additionally, there was strong labelling of punctate structures scattered throughout the cytoplasm (arrowheads in panel b) and a weaker reticular labelling extending out to the periphery of the cells. In the presence of rifampin, anti-p32 strongly labels the rifampin bodies (arrowheads in panel e) as defined in phase-contrast microscopy (arrowheads in panel f). Again, there is a weaker reticular labelling throughout the whole cytoplasm.

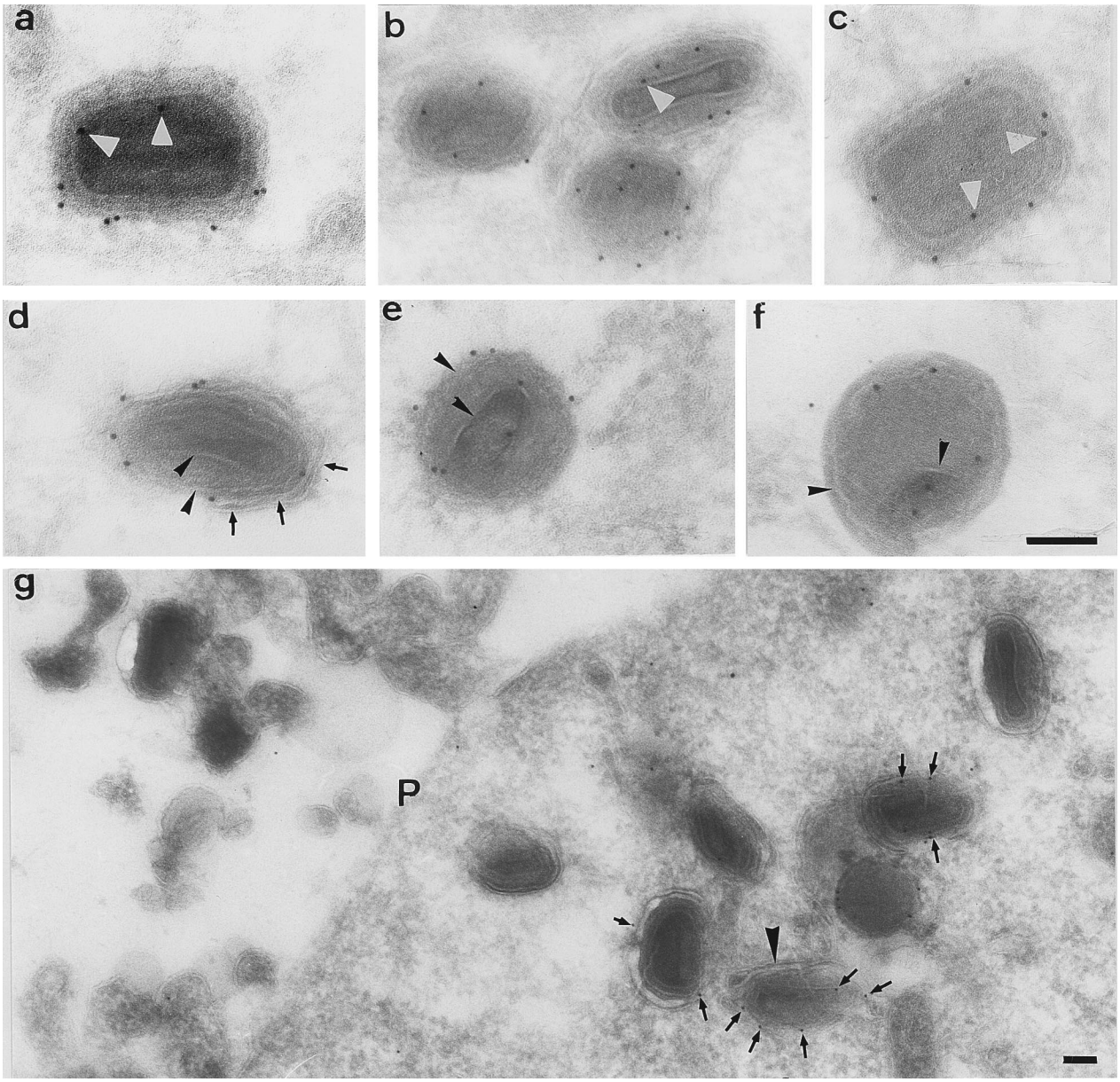

FIG. 2. EM immunogold localization of p32. Cryosections of vaccinia virus-infected HeLa cells at 8 h postinfection were labelled with anti-p32 antibody followed by protein A-gold. In panels a to c, labelling of IMV is shown. Most of the gold particles are associated with the outer membrane of the IMV; the arrowheads indicate label that appears to be associated with the inner membrane. In panel d, a p32-labelled IMV is partially enwrapped by a membrane cisterna (arrows); the arrowheads show the two membranes of the IMV. In panels e and f, intermediate-stage (between IV and IMV) particles are shown. The arrowheads indicate the two membranes. Note that some label is associated with the inner membrane. In panel g, a peripheral part of the cell is shown that contains a number of IEV profiles (the arrowhead indicates a cisterna that is tightly opposed to an IEV particle). Note that some of the IEVs are labelled significantly (small arrows), while others are unlabelled. Bars, 100 nm.

were clearly labelled by anti-p32 (Fig. 6a, c, and d). The electron-dense, irregularly shaped crystalloid structures containing DNA were invariably not labelled (Fig. 5d). The Golgi stacks, the plasma membrane (not shown), the mitochondria, and all other cell organelles had only occasional gold particles, which we assume to be background labelling (Fig. 6a). There was also a low labelling of the ER and nuclear envelope (not shown). When cells were incubated in drug-free medium for short time periods after the rifampin treatment, there was a synchronous assembly of viral crescents from the rifampin bodies (19, 46). As shown in Fig. 6b, when rifampin was chased for 15 min, there was significant labelling for p32 in the viral crescents which formed from the rifampin bodies.

Localization of p14. The second well-characterized membrane protein of the IMV that we investigated was p14 (6, 16, 37, 38, 40). In all our experiments, both anti-p14 antibodies that we have used gave identical results. By immunofluorescence microscopy at 4 h after vaccinia virus infection, anti-p14 gave a diffuse cytoplasmic labelling which did not show any reticular-like appearance (not shown). At 8 h postinfection, anti-p14 additionally labelled many distinct punctate structures, most probably single IMV particles, which accumulated

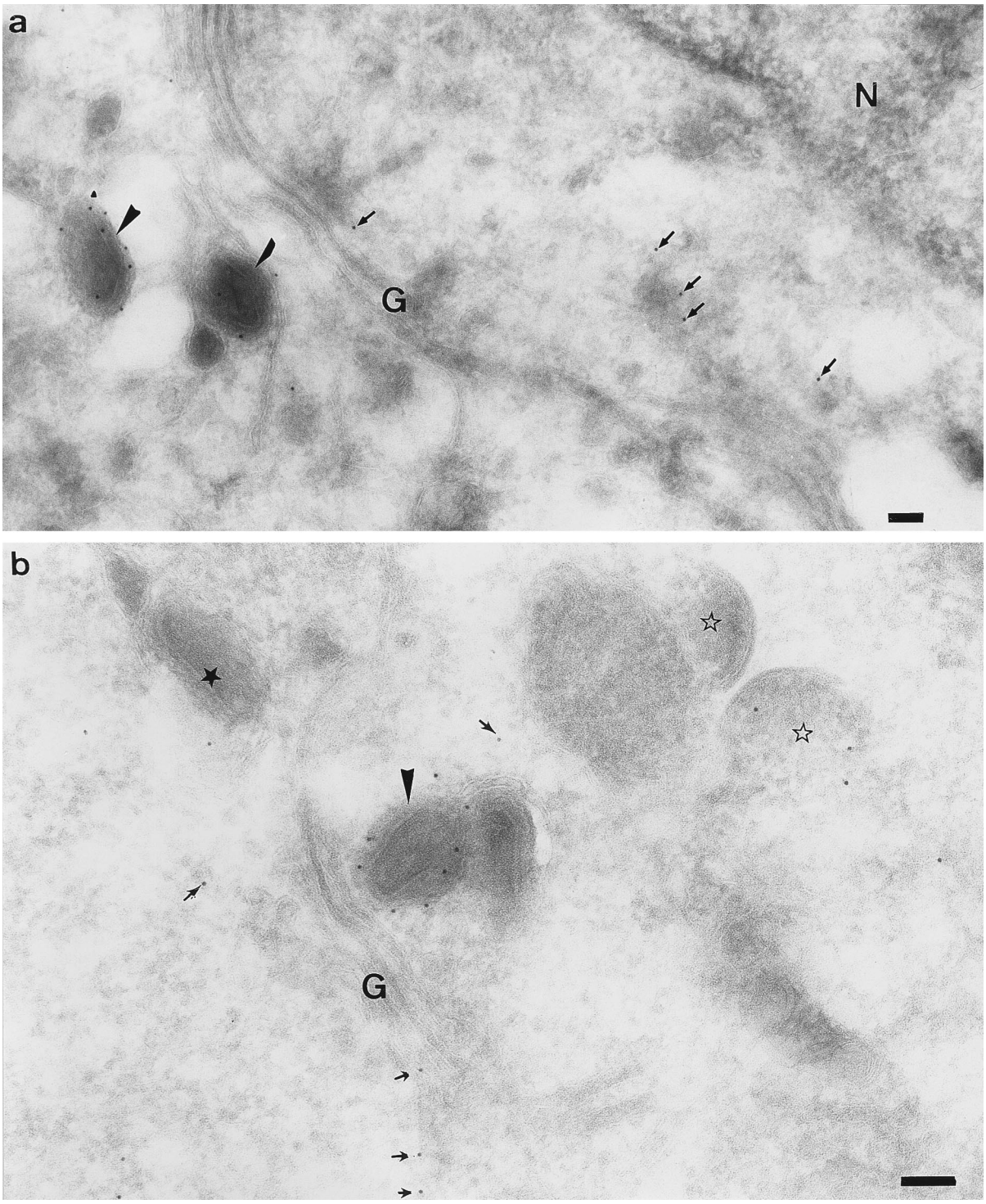

FIG. 3. Labelling for p32 in the perinuclear region of HeLa cells at 8 h postinfection. In addition to labelling, the IMV (arrowheads) gold particles are also associated with the peripheral elements of the Golgi complex (G, small arrows). Note that one of the IVs (open stars) and one IMV (filled star) are devoid of labelling. N, nucleus. Bars, 100 nm.

predominantly in the perinuclear region, as well as larger, discrete structures that were the most prominent labelled elements in these cells (Fig. 7B, asterisk in inset). These structures are most likely accumulated virions. In very flat cells, it is evident that they are made up of groups of particles (not shown). In such cells, it was also evident that these larger structures were not coincident with the viral factories, as defined by DNA staining (Fig. 7A and B; also insets). After even longer infection times, the diffuse cytoplasmic labelling as well as the number of labelled punctate structures increased (not

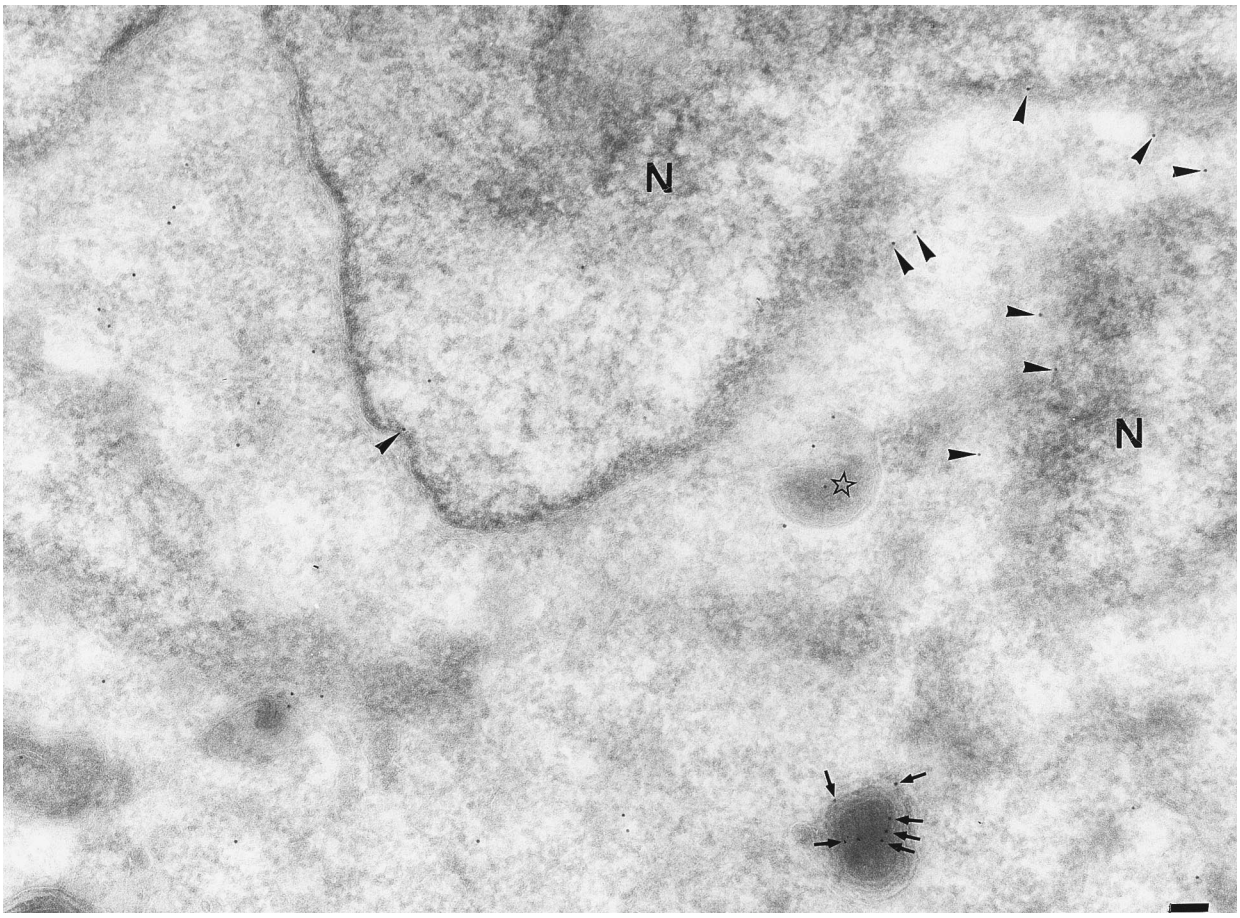

FIG. 4. Low-magnification image of HeLa cells at 8 h postinfection labelled for p32. Note the label that is preferentially associated with the nuclear envelope (N, nucleus [arrowheads]) as well as scattered in the cytoplasm. Both the IV (star) and a partially enwrapped IMV (arrows indicate gold) are labelled with anti-p32. Bar, 100 nm.

shown). In the presence of rifampin, anti-p14 also labelled the cytoplasm as well as the morphologically distinct rifampin bodies (Fig. 7D) which we identified with phase-contrast microscopy (references 45 and 46 and data not shown). In all infected cells, both in the absence and in the presence of rifampin, we always observed some labelling for p14 in the nucleus (Fig. 7B and D) which was absent from noninfected cells (not shown). Since p14 has a relatively low molecular weight, it is possible that it diffuses through the nuclear pores into the nucleus. At the relatively early times of infection that we have used in this study, we never observed any labelling of the plasma membrane (Fig. 6b and d). This was also the case when the immunofluorescence microscopy was carried out without cell permeabilization prior to labelling (not shown).

Immunoelectron microscopy experiments confirmed that the punctate labelling seen in control cells by immunofluorescence microscopy was due mainly to IMV particles (Fig. 8 and 9). Anti-p14 did not significantly label the IV (Fig. 8 and 9). However, an electron-dense intermediate form (45, 46) between the IV and the IMV form was strongly labelled predominantly on its outer membrane (Fig. 9). In general, the labelling of the IEV was variable. Figure 9e shows an example with significant labelling of the inner membranes. It seems likely that in the IEV the epitopes recognized by the antibodies are at least in part not accessible because of the binding of the additional membrane cisterna. We obtained similar results when we labelled cryosections of purified IMV or EEV particles. The purified IMVs were also labelled for p14 predominantly on their outer membrane with little associated with the inner membrane, whereas the intact EEVs were mostly devoid of labelling (data not shown). There was no obvious labelling of the plasma membrane or other cellular membranes, but there was often a low diffuse labelling over the cytoplasm (not shown). The overall pattern of p14 labelling, that is, no or very little labelling of viral crescents or IVs and strong labelling of intermediate forms and IMV, was fully confirmed with the SLO-permeabilized cells (Fig. 10). This argues against the possibility that the IVs were simply inaccessible to anti-p14 antibody.

In the presence of rifampin, the viral precursor membranes surrounding the rifampin bodies were strongly labelled by anti-p14 (Fig. 11b). Although there was always a low cytoplasmic labelling (Fig. 11b), the DNA crystalloids (D in Fig. 11c) were never labelled. When rifampin was washed out and the cells were chased in normal medium for 15 min, the viral crescents themselves were not labelled whereas the membranes connecting these viral crescents to the electron-dense rifampin bodies were positive for p14 (Fig. 11d). It remains to be established how p14 is excluded from the crescents during their formation. After longer chase times, the electron-dense intermediate form and the IMV were both strongly labelled by anti-p14 (data not shown).

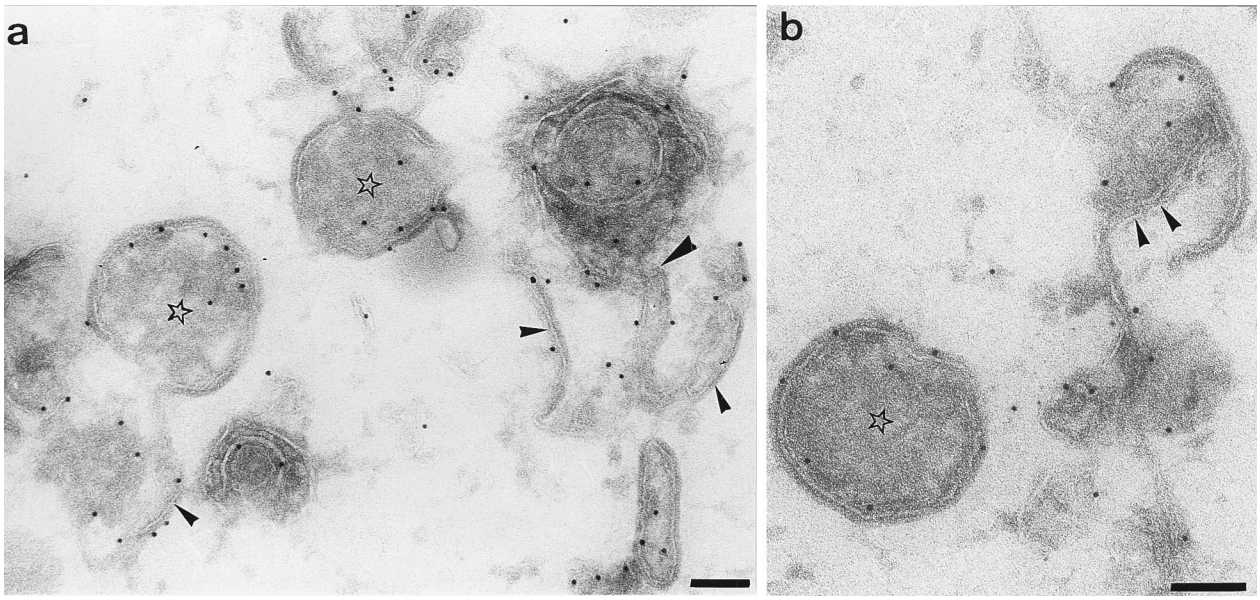

FIG. 5. Labelling of thawed cryosections of SLO-permeabilized HeLa cells at 8 h postinfection with p32. After the SLO permeabilization, the cytoplasm is extracted, and on the sections, there is a much higher degree of access for the anti-p32 antibody. Most of this label is membrane associated. The small arrowheads in panel a show labelling of viral crescent while the large arrowhead indicates a continuity between crescent membranes and an electron-dense membrane structure. Note the labelled membranes that appear to be partially enclosed by the developing crescent (arrowheads in panel b). Bars, 100 nm.

We also carried out double labelling with anti-p32 and anti-p14 and two sizes of gold (Fig. 12). This analysis confirmed the results from the single labelling, with p32 labelling all viral forms and strong labelling for p14 seen only in the intermediate stages. The IMVs were uniformly double labelled for both antigens.

Whole-mount labelling of purified virions. We confirmed that both p14 and p32 were exposed on the outside of the IMV by labelling whole virions with antibodies and gold before visualizing the virions by negative staining. Both antibodies gave a strong reaction in untreated virions (Table 1), and as expected, the label was essentially all abolished when the virions were treated with either trypsin (50 μg/ml, 37°C) or proteinase K (50 μg/ml, 4°C) (Table 1). When the virions were subjected to a variation of the treatment with NP-40 and reducing agent which has been widely used to separate envelope from cores (here, 1% NP-40 and 20 mM DTT [11, 21, 33, 43]), all the label for p14 and the bulk of label for p32 were removed relative to the untreated control. A surprising result came from pretreatment of the virus with 20 mM DTT alone before labelling. In the case of p32, this led to a loss of roughly half the label relative to the control. However, with p14 an almost fourfold increase was seen. A roughly twofold increase (≈80 gold particles per virion) was also seen when 1% mercaptoethanol was used instead of DTT (results not shown).

DISCUSSION

During the assembly of the first infectious form of vaccinia virus, at least four distinct morphological forms can be distinguished: the viral crescents, the IV, an electron-dense intermediate form, and the IMV itself (5, 13, 45). Our recent data indicate that the membranes of the crescents, the precursors of the IMV, originate from the intermediate compartment between the ER and the Golgi complex. This conclusion is based both on the existence of membrane continuities between the viral crescents and cellular membranes of the intermediate compartment and on the phospholipid composition of purified IMV particles (45). Vaccinia virus morphogenesis is clearly a complex, multistep process in which a large number of polypeptides must be assembled in a precise order to form a virus particle. The subviral localization of key structural proteins has, until now, relied mostly on the biochemical fractionation of purified IMV. Accordingly, the IMV proteins have been classified only as either detergent soluble, operationally defining the membrane proteins, or as detergent-insoluble, "core" proteins (e.g., see references 11, 21, 33, and 43).

To explain the crescent formation from membranes of the intermediate compartment, we propose the following working hypothesis: the formation of a specialized cisternal domain of the intermediate compartment is initiated by targeting vaccinia virus-encoded transmembrane proteins from the site of their synthesis, the rough ER, to the intermediate compartment where they are retained and therefore accumulate. We further envisage the crescent formation to be caused by an aggregation of these vaccinia virus membrane proteins, a process that is accompanied by an exclusion of cellular proteins. We further speculate that two kinds of protein-protein interaction would be involved in this process: first, lateral interactions within each membrane of a cisterna, and second, lumenal interactions which glue the two membranes together. All these processes are probably facilitated by vaccinia virus-encoded, peripheral membrane proteins. One obvious candidate for the latter is the vaccinia virus protein p65, the target of the drug rifampin, which is localized on the inner, concave, side of the crescents (46). The immunolocalization of the vaccinia virus proteins p32 and p14 in our present study should now be considered in the context of our assembly model.

p32, the product of the gene D8L, has all the hallmarks of a transmembrane protein, both from its predicted protein sequence and from its biochemical characterization (1a, 26, 32). On the basis of our immunogold labelling pattern for p32, we suggest that this protein is made in the rough ER membrane and subsequently transported to the intermediate compartment, where it is incorporated into the viral crescents. Bio-

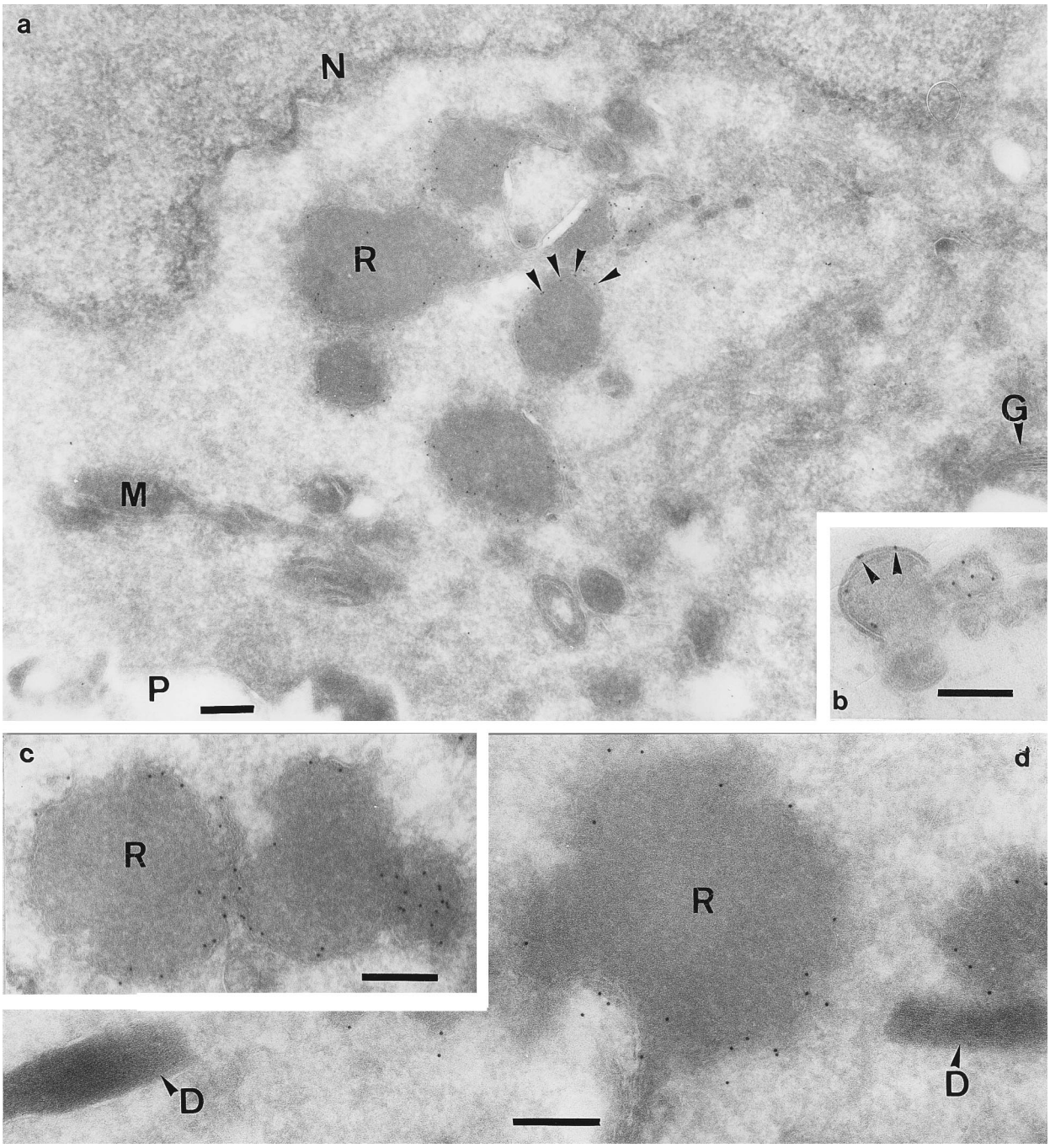

FIG. 6. Immunolocalization of p32 in cells infected in the presence of rifampin and after rifampin chase. Cryosections of HeLa cells infected with vaccinia virus (8 h) in the presence of rifampin (a, c, and d) and after chase of rifampin for 15 min (b) at 8 h postinfection were labelled with anti-p32 antibody. This antibody strongly labels the membranes (arrowheads) around the rifampin bodies (R in panels a, c, and d). Additionally, there is weak but significant labelling of cytoplasmic membranes but not the Golgi stacks (G in panel a), the plasma membrane (P in panel a), the mitochondria (M in panel a), or the DNA crystalloids (D in panel d). When rifampin is washed out, the viral crescents which assemble from the rifampin bodies are also labelled (arrowheads in panel b). N, nucleus. Bars, 200 nm.

chemical experiments are now in progress to try to confirm this working hypothesis. p32 was also localized in this study to the IV and the electron-dense intermediate form and, as expected, was found on the outer membrane of the IMV. The labelling of the IV was best demonstrated in cryosections of cells that had been permeabilized with SLO before fixation, a procedure which often improves access of antigens to their antibodies (25). When vaccinia virus assembly was blocked by rifampin, p32 accumulated on the viral precursor membranes associated with the rifampin bodies.

Collectively, these results agree with previous studies which have suggested that p32 is exposed on the outside of the IMV since a relatively large domain is removed by trypsin treatment of purified IMV (26, 32) and since some anti-p32 antibodies are neutralizing (2, 31a). Moreover, the p32 antibody labels intact IMV with immunogold followed by negative staining,

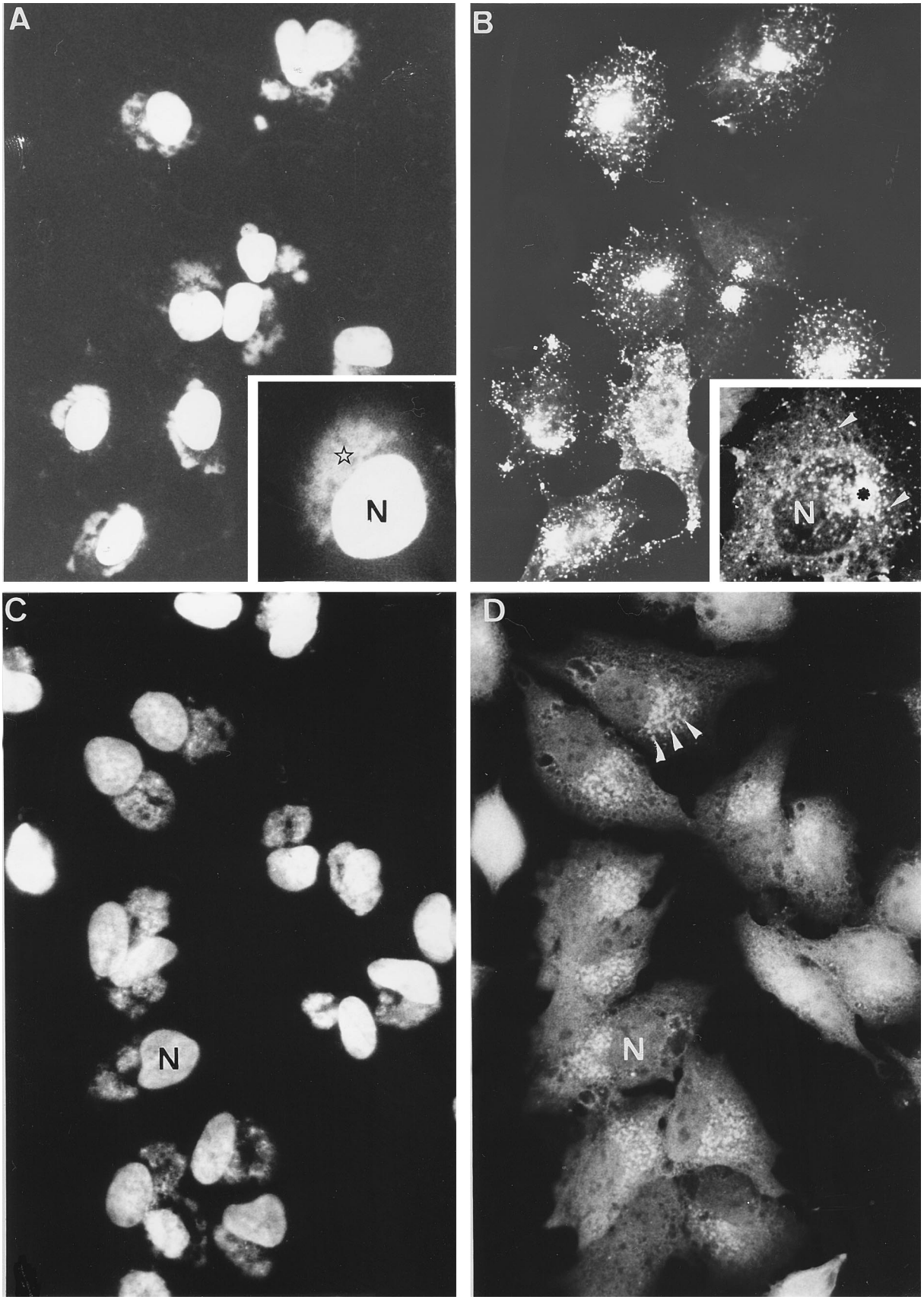
A
N
B
N
C
N
D
N

FIG. 7. Localization of p14 by immunofluorescence. Shown are vaccinia virus-infected HeLa cells 8 h postinfection in the absence (A and B) or presence (C and D) of rifampin. The cells were labelled with a fluorescent DNA dye (A and C) and with anti-p14 antibody followed by rhodamine-conjugated goat anti-rabbit antibody (B and D). In the absence of rifampin (B), anti-p14 gives a weak labelling of the cytoplasm and a strong labelling of punctate structures, probably individual virions, which accumulate in the perinuclear region (arrowheads) but which are also diffusely distributed throughout the cytoplasm, as is evident in the inset. The bulk of p14 labelling (asterisk in inset B) is clearly separated from the bulk of DNA (star in inset A). In the presence of rifampin (D), p14 accumulates on the rifampin bodies (arrowheads) easily identified in phase-contrast microscopy (not shown). The labelling of the cytoplasm in the presence of rifampin is stronger than in its absence (compare panel D with panel B). At these relatively early times of infection, there is no obvious labelling of the plasma membrane. N, nucleus.

and this label was essentially all lost when the virions were treated with proteases (Table 1). Additionally, it has been suggested that this protein functions as a ligand that facilitates the binding of IMV to the plasma membrane of susceptible cells (26, 27). In our EM sections, we also saw low but significant labelling for p32 on the inner membrane of the IMV, that is, the membrane that appears to be most closely associated with the DNA core (e.g., Fig. 2c and e). The significance of this observation awaits more detailed studies of the assembly process.

In contrast to p32, the amino acid sequence of p14 predicts a protein that lacks a putative signal sequence and a transmembrane domain. It contains only two very short, hydrophobic stretches: one of 5 amino acids at the amino terminus and one of 11 at the carboxy terminus (38). Our immunolocalization studies showed that, unlike p32, p14 was acquired at a distinct and later step of vaccinia virus assembly. Thus, while the early morphological forms of vaccinia virus were devoid of p14, there was strong labelling of the electron-dense intermediate form as well as the IMV. Importantly, and again in contrast to p32, most, if not all of the label for p14 was associated with the outer membranes of both the intermediate and the IMV forms. These observations are consistent with other data showing that p14 must be exposed on the outside of the IMV. Thus, some anti-p14 antibodies are neutralizing for IMV but not for EEV infection (6, 39). Further, this protein appears to be involved in the fusion of the IMV with the plasma membrane of the host cell (6, 16) and is essential for the intracellular wrapping of the IMV to form the IEV (41). That p14 is on the outside of IMV in significant amounts was also confirmed by labelling whole IMV with immunogold labelling followed by negative staining; almost all of this label is lost

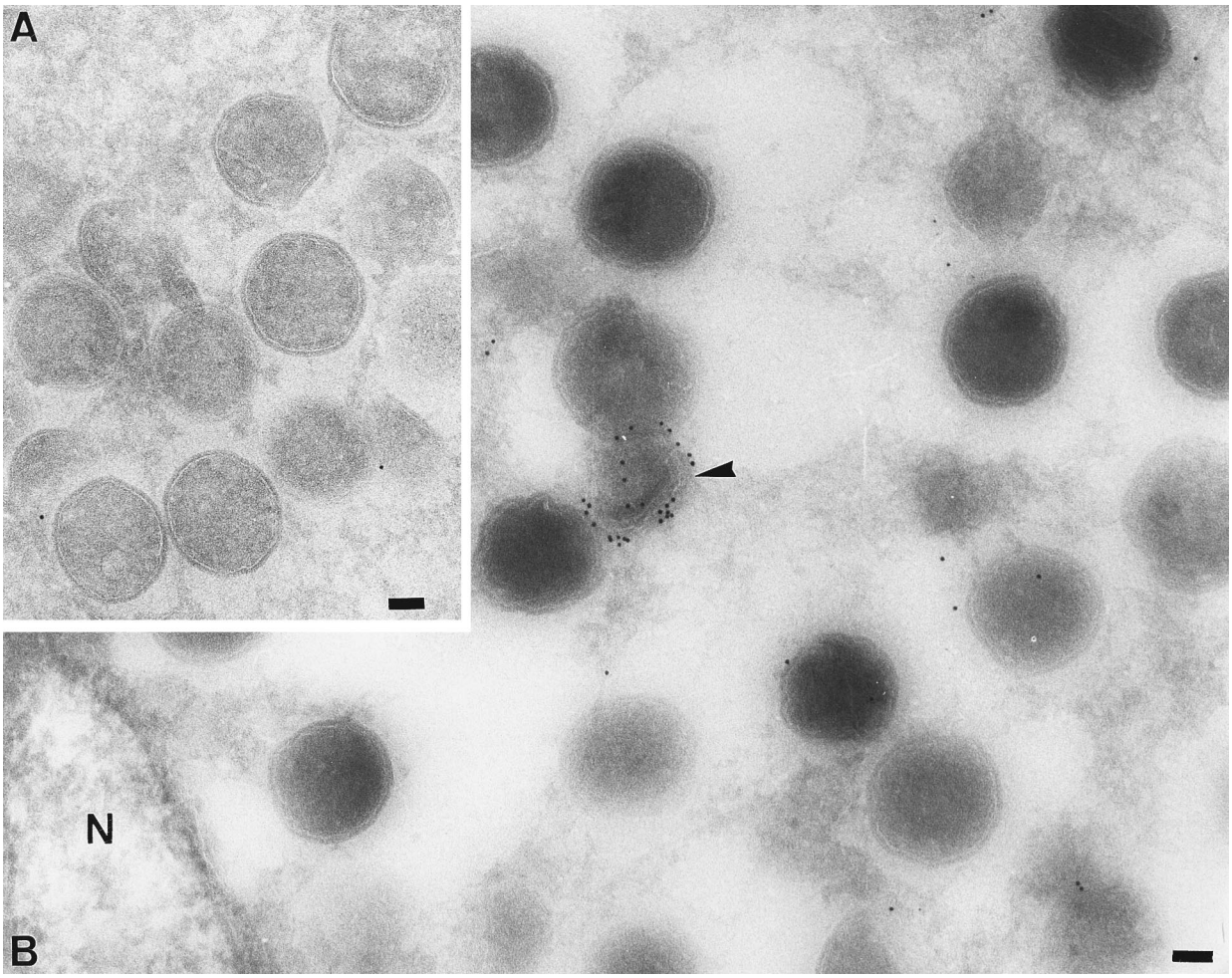

FIG. 8. EM immunolocalization of p14 in vaccinia virus-infected HeLa cells at 8 h postinfection. Most of the spherical IVs are either completely devoid of labelling or have a few single gold particles. In contrast, the IMV (arrowhead in panel B) is strongly labelled. N, nucleus. Bars, 100 nm.

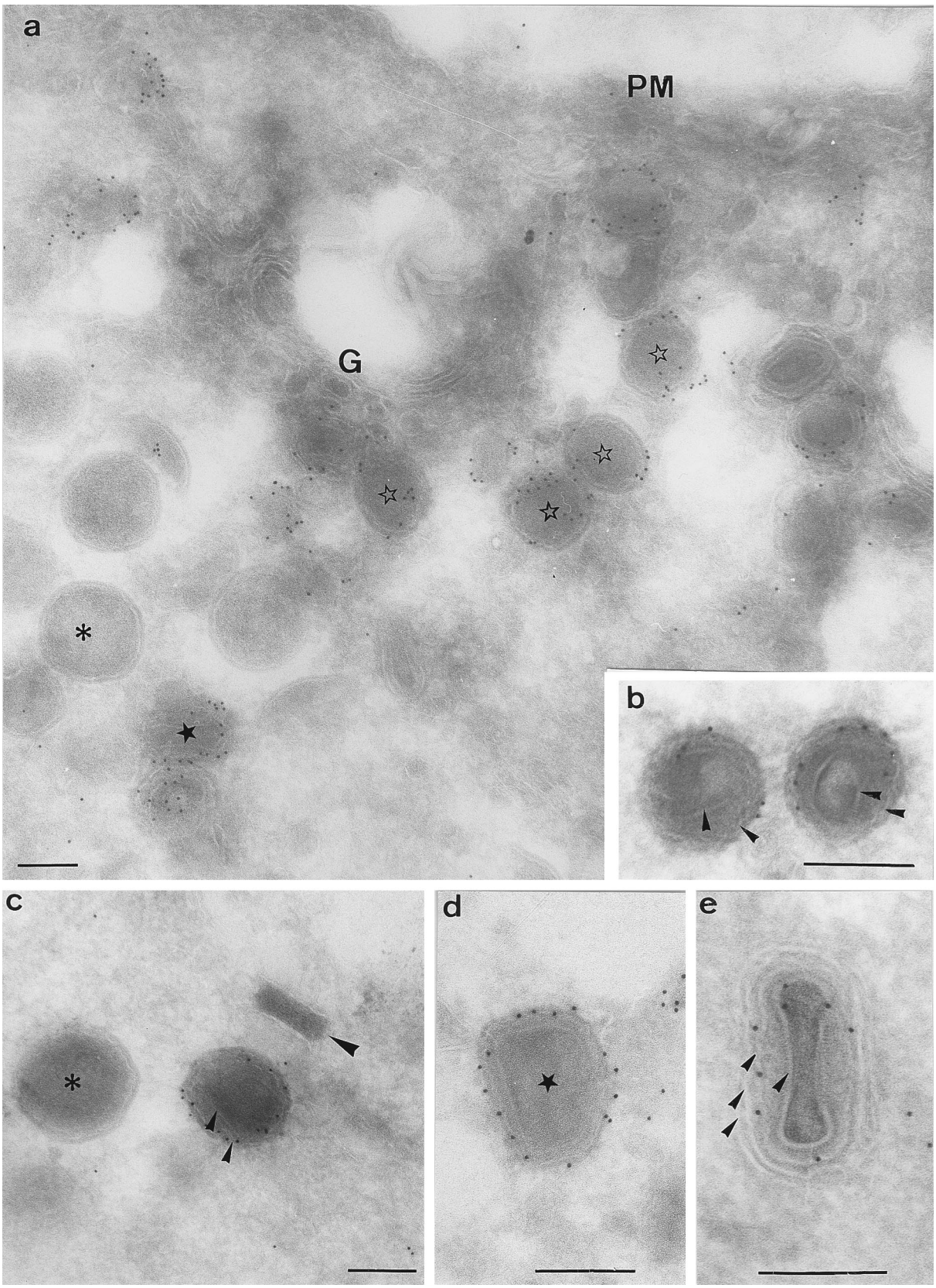

FIG. 9. EM immunolocalization of p14. Shown are cryosections of vaccinia virus-infected BHK cells at 10 h postinfection (a) and HeLa cells at 8 h postinfection (b to e). Anti-p14 does not label the immature virions (asterisks in panels a and c). The spherical intermediate form between the IV and the IMV, characterized by an outer membrane and a second, internal membrane around the core (arrowheads in panels b and c), is clearly labelled on its outer membrane. In some cases, a more electron-dense form of the IV (open stars in panel a) shows a strong labelling for p14. These forms presumably represent a stage just prior to the stages shown in panel a. The IMV (filled star in panels a and d) is strongly labelled on its outer membrane but not on its inner membrane. In panel e, an IEV particle is shown with its four distinct membranes (arrowheads); note that the labelling is restricted to the inner membranes. Large arrowhead in panel c, viral DNA. Bars, 200 nm.

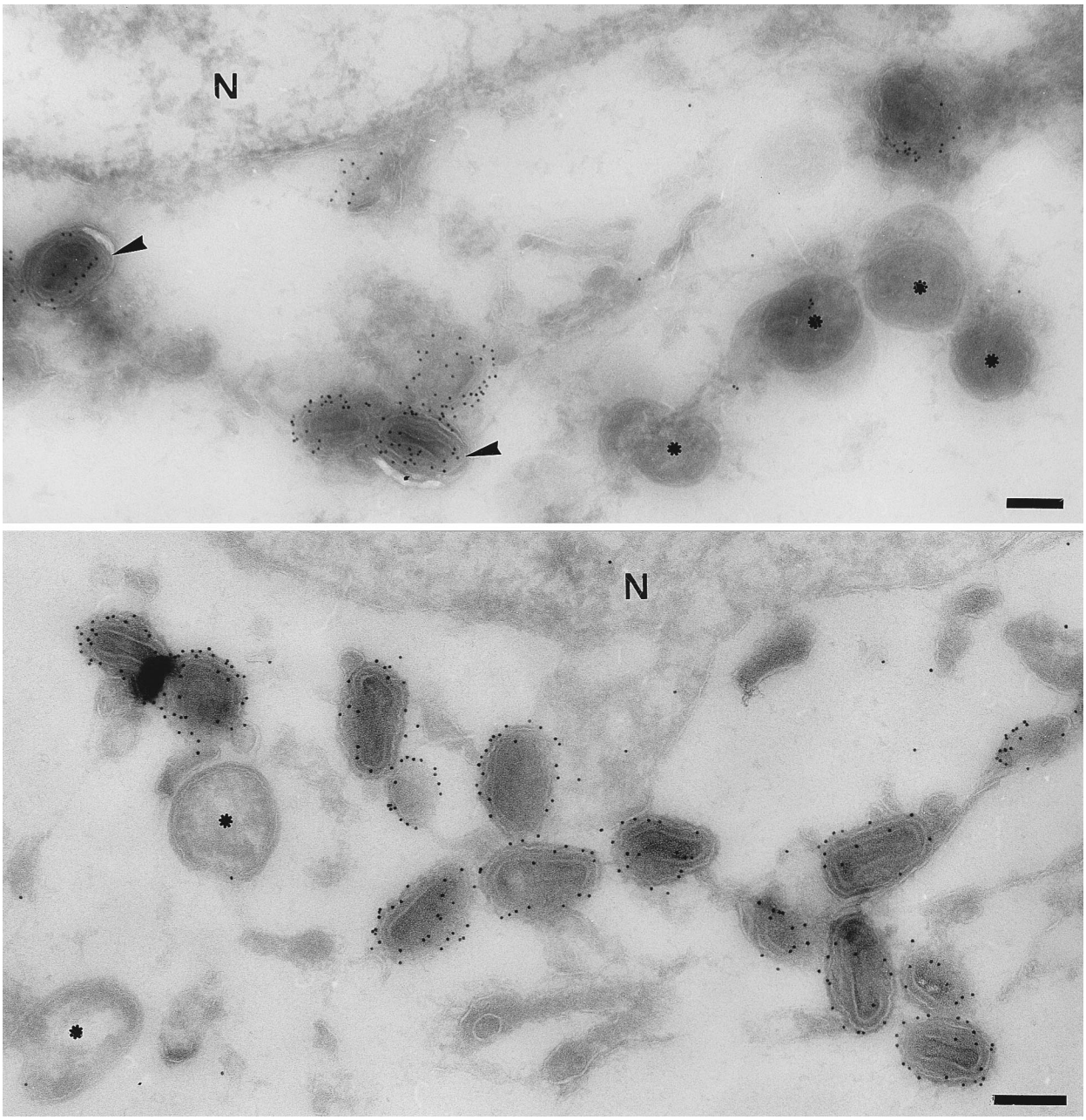

FIG. 10. Labelling of SLO-permeabilized, vaccinia virus-infected HeLa cells at 8 h postinfection with anti-p14 antibody. Even under this condition, the majority of IV particles (asterisks) have essentially no label while the IMV particles are strongly labelled on their periphery. The nuclear membrane (N, nucleus) is not labelled. Bars, 100 nm.

following treatment of the IMV with proteases (Table 1). Finally, upon treatment of [^{35}S]methionine-labelled IMV with proteinase K the band for p14 in sodium dodecyl sulfate-polyacrylamide gel electrophoresis is completely lost (unpublished data).

Collectively, the data are consistent with a model whereby p14 is synthesized on free cytoplasmic ribosomes and associates posttranslationally with the cytoplasmic domain of a membrane receptor. We propose that this putative membrane receptor becomes inserted into the early crescent but would only become active for binding p14 at the transition stage from the IV to the electron-dense intermediate form. The viral precursor membranes associated with the rifampin bodies were also labelled by anti-p14. Possibly, in the presence of rifampin, a significant amount of the putative p14 receptor in its active form might accumulate on the membranes of the rifampin bodies, but only the inactive form would be found on the crescents which form after washout of the drug. It remains to be determined whether or not the p14 which accumulates on these rifampin body membranes can be subsequently incorporated into IMV. One candidate for a p14 receptor is the 21-kDa protein, encoded by the gene A17L, which can be coprecipitated with antibodies directed to p14 (37). Since the amino acid sequence of A17L predicts two large internal hydrophobic

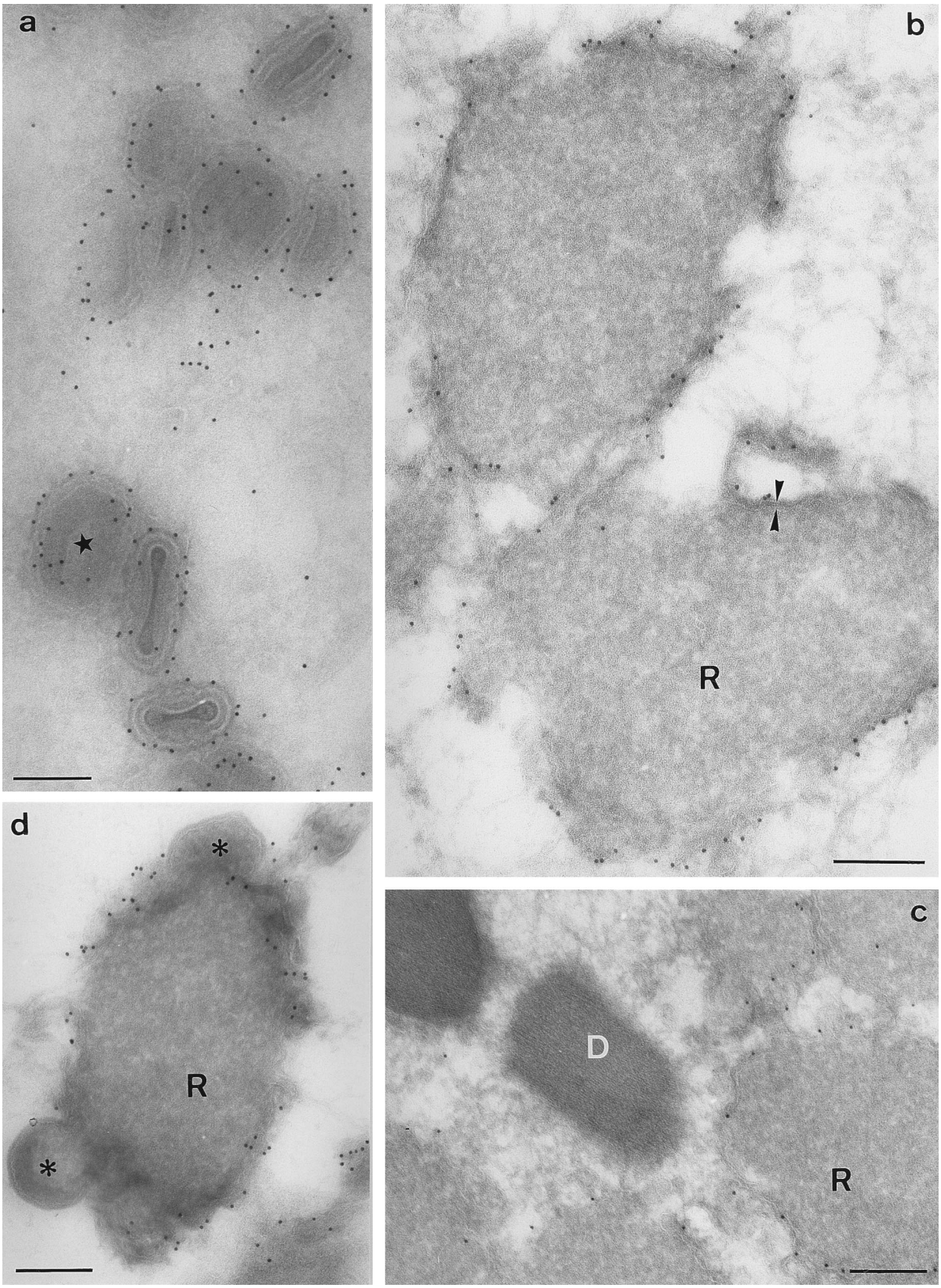

FIG. 11. Immunolocalization of p14 in the IMV and in cells infected in the presence of rifampin. Cryosections of vaccinia virus-infected HeLa cells at 15 h postinfection (a) and 8 h postinfection (b and c) and BHK cells (d) at 10 h postinfection were labelled with anti-p14 antibody. The cells in panels b and c were treated with rifampin, and those in panel d were treated with rifampin followed by a 15-min chase. Anti-p14 strongly labels the outer membrane of the IMV (a). In the presence of rifampin, p14 accumulates on the membranes (arrowheads in panel b) of the rifampin bodies (R) but is invariably absent from the viral crescents (asterisks in panel d) that are continuous with the membranes of the rifampin bodies. In panel c, the DNA-enriched crystalloid bodies (D) are not labelled for p14. Bars, 200 nm.

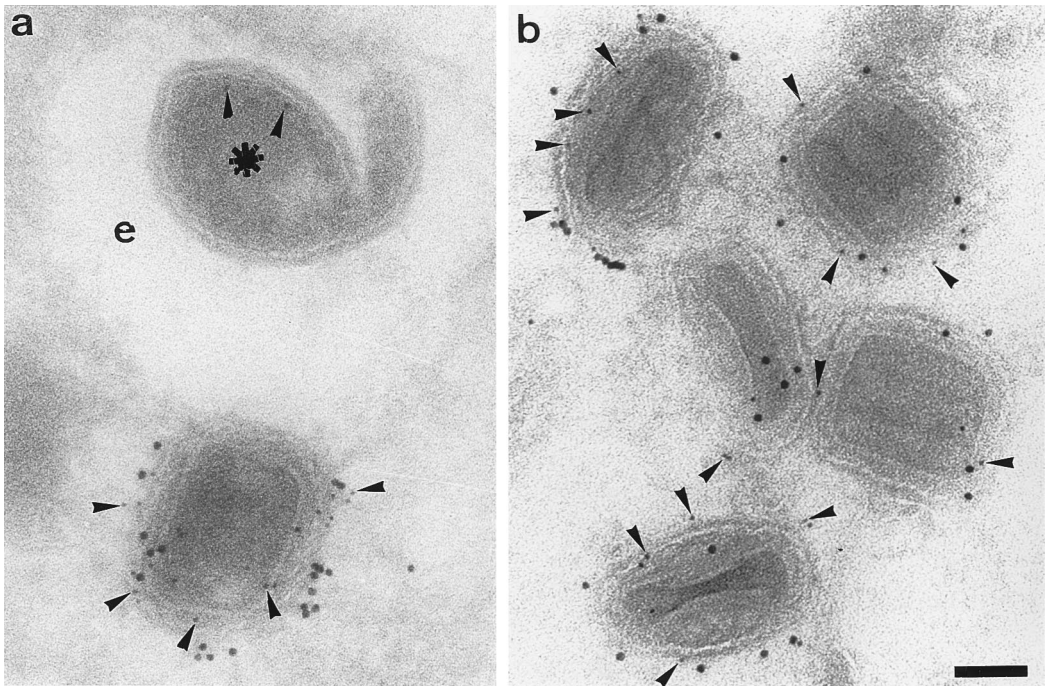

FIG. 12. Double labelling of HeLa cells at 8 h postinfection with anti-p32 (5-nm gold; arrowheads) and anti-p14 (10-nm gold). The IV (asterisk) has two gold particles for p32 but is not labelled for p14. On average, every IMV particle has at least some label for both antigens. Bar, 100 nm.

domains characteristic for membrane proteins, an interaction with this protein would provide a means to anchor p14 to the membrane (37).

Two previously published observations concerning p14 are difficult to reconcile with our data. First, earlier immunofluorescence experiments showed labelling of unpermeabilized cells, suggesting that p14 is localized on the extracellular face of the plasma membrane (40). This difference from our data might be explained by the later time points used in the previous study, when more severe cytopathic effects of the vaccinia virus infection might be expected. Second, it was shown that this protein exists in purified virions as disulfide-linked trimers (40). In our assembly model, p14 is located on the cytoplasmic surface of the IMV particles. Since the redox state of the cytoplasm is highly reducing (8, 14, 20, 22), we consider it unlikely that disulfide bonds, which can only form intracellularly in the oxidative environment of the ER, would form between p14 molecules on the intracellular IMV. Most likely, these bonds would be formed either in the oxidizing extracellular environment after the secretion of EEV or after the IMVs have been released by cell lysis. In the former case, an interesting possibility to consider would be that the oxidation of p14 in the extracellular space might be a prerequisite for this protein to become fusion competent.

TABLE 1. Labelling of intact, purified IMV

Treatment before labelling[a]	Gold particles/virion (mean ± SD)			
	p14		p32	
	No.[b]	%[c]	No.[d]	%[c]
Untreated	39.4 (4.8)	100	17.8 (4.2)	100
NP-40 (1%)–DTT (20 mM)	0.5 (0.6)	1.2	7.0 (2.1)	39.3
DTT (20 mM)	140 (12)	355.3	7.5 (6.5)	42.1
Trypsin (50 μg/ml)	0.9 (0.8)	2.3	3.1 (2.1)	17.4
Proteinase K (50 μg/ml, 4°C)	0.9 (0.9)	2.3	0.6 (0.8)	3.4

[a] In each case, the virions were adsorbed onto Formvar- and carbon-coated grids and treated for 30 min at 37°C.
[b] Labelled by a three-step protocol: the monoclonal anti-p14 (1) was labelled by rabbit anti-mouse antibody (3) followed by protein A-gold (10 nm).
[c] For the percentages, the values for untreated virus are normalized to 100%.
[d] Labelled by a two-step protocol: the rabbit anti-N terminus of p32 was visualized by protein A-gold (10 nm).

If p14 is on the cytoplasmic (outer) surface of IMV, how do we explain the fact that treatments which reduce disulfide bonds (Table 1) lead to a significant increase in surface labelling with anti-p14? The first explanation is based on the supposition that p14 has indeed formed disulfide-bonded trimers in the extracellular milieu, as discussed above. Breaking these bonds could provide greater access of the antibody to its antigen. An alternative possibility is that the S-S bonds are strictly lumenal and that DTT weakens the association between the outer and inner virion membranes such that the p14 on the opposite side of the outer membrane now becomes more accessible. That DTT loosens the contact between the outer and inner membrane is supported by cryo-EM images of DTT-treated IMV (42a).

The presence of neither p14 nor p32 is not obligatory for IMV production in cell culture (27, 32). Thus, besides the peripheral membrane protein p65 (48), no other viral membrane or membrane-associated proteins have yet been identified that are essential for the formation of the membrane crescents or for the morphogenetic changes leading to the IMV. Other transmembrane proteins which may be involved are the 21-kDa protein (37) and the putative p65 receptor (46). The complete sequencing of the vaccinia virus genome has predicted at least 30 further putative integral membrane proteins (15), which remain to be characterized. Our immediate goal is to determine which of these membrane proteins are

essential for the formation of the IV (IMV) and, more importantly, to elucidate how a macromolecular complex of the virus is able to assemble the crescents and the IV.

ACKNOWLEDGMENTS

We thank Kai Simons and Jacomine Krijnse Locker (EMBL) for many stimulating discussions during the course of this work. We also thank Rafael Blasco for critical evaluation of the manuscript. The manuscript was typed by Julia Pickles.

REFERENCES

1. **Cairns, H. J. F.** 1960. The initiation of vaccinia infection. Virology **11:**603.
1a. **Cudmore, S., and G. Griffiths.** Unpublished observations.
2. **Czerny, C. P., S. Johann, L. Hölzle, and H. Meyer.** 1994. Epitope detection in the intracellular naked orthopox viruses and identification of encoding genes. Virology **210:**764–767.
3. **Czerny, C. P., and H. Mahnel.** 1990. Structural and functional analysis of orthopoxvirus epitopes with neutralizing monoclonal antibodies. J. Gen. Virol. **71:**2341–2352.
4. **Dales, S.** 1963. The uptake and development of vaccinia virus in strain L cells followed with labelled viral deoxyribonucleic acid. J. Cell Biol. **18:** 51–72.
5. **Dales, S., and B. G. T. Pogo.** 1981. Biology of poxviruses. Virol. Monogr. **18**.
6. **Dallo, S., J. F. Rodriguez, and M. Esteban.** 1987. A 14K envelope protein of vaccinia virus with an important role in virus-host cell interactions is altered during virus persistence and determines the plaque size phenotype of the virus. Virology **159:**423–432.
7. **Doms, R. W., R. Blumenthal, and B. Moss.** 1990. Fusion of intracellular- and extracellular forms of vaccinia virus with the cell membrane. J. Virol. **64:** 4884–4892.
8. **Doms, R. W., R. A. Lamb, J. K. Rose, and A. Helenius.** 1993. Folding and assembly of viral membrane proteins. Virology **193:**545–562.
9. **Dubochet, J., M. Adrian, K. Richter, J. Garces, and R. Wittek.** 1994. Structure of intracellular mature vaccinia virus observed by cryoelectron microscopy. J. Virol. **68:**1935–1941.
10. **Earl, P. L., and B. Moss.** 1991. Expression of proteins in mammalian cells using vaccinia viral vectors, p. 16.19.1–16.19.10. *In* F. M. Ausubel et al. (ed.), Current protocols in molecular biology. Greene Publishing Associates and Wiley Interscience, New York.
11. **Easterbrook, K. B.** 1966. Controlled degradation of vaccinia virions *in vitro*: an electron microscopic study. J. Ultrastruct. Res. **14:**484–496.
12. **Essani, K., and S. Dales.** 1979. Biogenesis of vaccinia: evidence for more than 100 polypeptides in the virion. Virology **95:**385–394.
13. **Fenner, F., R. Wittek, and K. R. Dumbell.** 1989. The orthopoxviruses. Academic Press Inc., San Diego, Calif.
14. **Gething, M. J., and J. Sambrook.** 1992. Protein folding in the cell. Nature (London) **355:**33–45.
15. **Goebel, S. J., G. P. Johnson, M. E. Perkus, S. W. Davis, J. P. Winslow, and E. Paoletti.** 1990. The complete DNA sequence of vaccinia virus. Virology **179:**247–266.
16. **Gong, S., C. Lai, and M. Esteban.** 1990. Vaccinia virus induces cell fusion at acid pH and this activity is mediated by the N-terminus of the 14kDa virus envelope protein. Virology **178:**81–91.
17. **Griffiths, G.** 1993. Fine structure immunocytochemistry. Springer-Verlag, Heidelberg, Germany.
18. **Griffiths, G., and P. Rottier.** 1992. Cell biology of viruses that assemble along the biosynthetic pathway. Semin. Cell Biol. **3:**367–381.
19. **Grimley, P. M., E. N. Rosenblum, S. J. Mims, and B. Moss.** 1970. Interruption by rifampin of an early stage in vaccinia virus morphogenesis: accumulation of membranes which are precursors of virus envelopes. J. Virol. **6:**519–533.
20. **Helenius, A., T. Marquardt, and I. Braakman.** 1992. The endoplasmic reticulum as a protein-folding compartment. Trends Cell Biol. **2:**227–231.
21. **Holowczak, J. A., and W. K. Joklik.** 1967. Studies of the structural proteins of virions and cores. Virology **33:**717–725.
22. **Hwang, C., A. J. Sinskey, and H. F. Lodish.** 1992. Oxidized redos state of glutathione in the endoplasmic reticulum. Science **257:**1496–1992.
23. **Ichihashi, Y., M. Oie, and T. Tsuruhara.** 1984. Location of DNA-binding proteins and disulfide-linked proteins in vaccinia virus structural elements. J. Virol. **50:**929–938.
24. **Joklik, W. K., and Y. Becker.** 1964. The replication and coating of vaccinia DNA. J. Mol. Biol. **10:**452–474.
25. **Krijnse-Locker, J., M. Ericsson, P. J. M. Rottier, and G. Griffiths.** 1994. Characterization of the budding compartment of mouse hepatitis virus: evidence that transport from the RER to the Golgi complex requires only one vesicular transport step. J. Cell Biol. **124:**55–70.
26. **Lai, C., S. Gong, and M. Esteban.** 1991. The 32-kilodalton envelope protein of vaccinia virus synthesized in *Escherichia coli* binds with specificity to cell surfaces. J. Virol. **65:**499–504.
27. **Maa, J. S., J. F. Rodriguez, and M. Esteban.** 1990. Structural and functional characterization of a cell surface binding protein of vaccinia virus. J. Biol. Chem. **265:**1569–1577.
28. **Moss, B.** 1991. Vaccinia virus: a tool for research and vaccine development. Science **252:**1662–1667.
29. **Moss, B., and E. N. Rosenblum.** 1973. Protein cleavage and poxvirus morphogenesis: tryptic peptide analysis of core precursors accumulated by blocking assembly with rifampicin. J. Mol. Biol. **81:**267–269.
30. **Moss, B., E. N. Rosenblum, and E. Katz.** 1969. Rifampicin: a specific inhibitor of vaccinia virus assembly. Nature (London) **224:**1280–1284.
31. **Nagayama, A., B. G. T. Pogo, and S. Dales.** 1970. Biogenesis of vaccinia: separation of early stages from maturation by means of rifampicin. Virology **4:**1039–1051.
31a. **Niles, E. G.** Unpublished observations.
32. **Niles, E. G., and J. Seto.** 1988. Vaccinia virus gene D8 encodes a virion transmembrane protein. J. Virol. **62:**3772–3778.
33. **Oie, M., and Y. Ichihashi.** 1981. Characterization of vaccinia polypeptides. Virology **113:**263–276.
34. **Oie, M., and Y. Ichihashi.** 1987. Modification of vaccinia virus penetration proteins analyzed by monoclonal antibodies. Virology **157:**449–459.
35. **Paez, E., S. Dallo, and M. Esteban.** 1987. Virus attenuation and identification of structural proteins of vaccinia virus that are selectively modified during virus persistence. J. Virol. **61:**2642–2647.
36. **Payne, L. G., and K. Kristenson.** 1979. Mechanism of vaccinia virus release and its specific inhibition by N_1-isonicotinoyl-N_2-3-methyl-4-chlorobenzoylhydrazine. J. Virol. **32:**614–622.
37. **Rodriguez, D., J. R. Rodriguez, and M. Esteban.** 1993. The vaccinia virus 14-kilodalton fusion protein forms a stable complex with the processed protein encoded by the vaccinia virus A17L. J. Virol. **67:**3435–3440.
38. **Rodriguez, J. F., and M. Esteban.** 1987. Mapping and nucleotide sequence of the vaccinia gene that encodes a 14-kilodalton fusion protein. J. Virol. **61:**3550–3554.
39. **Rodriguez, J. F., R. Janeczko, and M. Esteban.** 1985. Isolation and characterization of neutralizing monoclonal antibodies to vaccinia virus. J. Virol. **56:**482–488.
40. **Rodriguez, J. F., E. Paez, and M. Esteban.** 1987. A 14,000-M_r envelope protein of vaccinia virus is involved in cell fusion and forms covalently linked trimers. J. Virol. **61:**393–404.
41. **Rodriguez, J. F., and G. F. Smith.** 1990. IPTG-dependent vaccinia virus: identification of a virus protein enabling virion envelopment by Golgi membrane and egress. Nucleic Acids Res. **18:**5347–5351.
42. **Rodriguez, J. R., D. Rodriguez, and M. Esteban.** 1992. Insertional inactivation of the vaccinia virus 32-kilodalton gene is associated with attenuation in mice and reduction of viral gene expression in polarized epithelial cells. J. Virol. **66:**183–189.
42a. **Roos, N., and G. Griffiths.** Unpublished data.
43. **Sarov, I., and W. K. Joklik.** 1972. Studies on the nature and location of the capsid polypeptides of vaccinia virions. Virology **50:**579–592.
44. **Schmelz, M., B. Sodeik, M. Ericsson, E. J. Wolffe, H. Shida, G. Hiller, and G. Griffiths.** 1994. Assembly of vaccinia virus: the second wrapping cisterna is derived from the trans Golgi network. J. Virol. **68:**130–147.
45. **Sodeik, B., R. W. Doms, M. Ericsson, G. Hiller, C. E. Machamer, W. van't Hof, G. van Meer, B. Moss, and G. Griffiths.** 1993. Assembly of vaccinia virus: role of the intermediate compartment between the endoplasmic reticulum and the Golgi stacks. J. Cell Biol. **121:**521–541.
46. **Sodeik, B., G. Griffiths, M. Ericsson, B. Moss, and R. W. Doms.** 1994. Assembly of vaccinia virus: effects of rifampin on the intracellular distribution of viral protein p65. J. Virol. **68:**1103–1114.
47. **Stern, W., and S. Dales.** 1976. Biogenesis of vaccinia: isolation and characterization of a surface component that elicits antibody suppressing infectivity and cell-cell fusion. Virology **75:**232–241.
48. **Zhang, Y., and B. Moss.** 1992. Immature viral envelope formation is interrupted at the same stage by lac operator-mediated repression of the vaccinia virus D13L gene as by the drug rifampicin. Virology **187:**643–653.